Equilibrium Behavior and Proton Transfer Kinetics of the Dioxotetracyanometalate Complexes of Molybdenum(IV), Tungsten(IV), Technetium(V), and Rhenium(V): Carbon-13 and Oxygen-17 NMR Study

Andreas Roodt,*[,1] Johann G. Leipoldt,[1] Lothar Helm,[2] and André E. Merbach*[,2]

Institut de Chimie Minérale et Analytique, Université de Lausanne, Place du Château 3, CH-1005 Lausanne, Switzerland, and Department of Chemistry, University of the Orange Free State, Bloemfontein 9300, South Africa

Received June 3, 1993[⊗]

The aqueous equilibrium and protonation kinetics of the protonated forms of the $[MO_2(CN)_4]^{(n+2)-}$ complexes for the Mo(IV) and W(IV) systems (pH 6–14), and the Tc(V) and Re(V) systems (pH 0–8), have been quantitatively studied by ^{13}C and ^{17}O NMR at 25.0 °C and μ = 1.0–1.4 *m* (KNO_3). The pK_{a1} values for the $[MO(OH_2)(CN)_4]^{2-}$ complexes for W(IV) and Mo(IV) were determined as 7.87(5) and 9.88(5). ^{17}O line broadening were simulated and proton exchange rate constants for the Mo(IV) and W(IV) systems were determined: (i) $[MO(OH)(CN)_4]^{3-} + OH^- \rightleftharpoons [MO_2(CN)_4]^{4-} + H_2O$ (k_{-2b}, k_{2b}); (ii) $[MO(OH_2)(CN)_4]^{2-} + [^*MO(OH)(CN)_4]^{3-} \rightleftharpoons [MO(OH)(CN)_4]^{3-} + [^*MO(OH_2)(CN)_4]^{2-}$ (k_{1ex}). In *strong basic* medium (pH > 11) for the Mo(IV) and W(IV) systems, the deprotonation rate constants (k_{-2b}) for the $[MO(OH)(CN)_4]^{4-}$ complexes were determined as 2(1) × 10^7 and 4(2) × 10^8 M^{-1} s^{-1}, while protonation rate constants (k_{2b}) for the $[MO_2(CN)_4]^{3-}$ complexes of 1.3(2) × 10^9 and 7(2) × 10^8 s^{-1} were obtained. In *weak basic* medium where hydrolysis of the aqua–oxo complex is less important, the lower limit of the direct proton exchange constant, k_{1ex}, was determined as 1 × 10^7 M^{-1} s^{-1} for both Mo(IV) and W(IV). Proton transfer in the Re(V) and Tc(V) systems can be described by (iii) $[MO(OH_2)(CN)_4]^- \rightleftharpoons [MO(OH)(CN)_4]^{2-} + H^+$ (k_{1a}, k_{-1a}); (iv) $[MO(OH)(CN)_4]^{2-} \rightleftharpoons [MO_2(CN)_4]^{3-} + H^+$ (k_{2a}, k_{-2a}); (v) $[MO(OH)(CN)_4]^{2-} + [^*MO_2(CN)_4]^{3-} \rightleftharpoons [MO_2(CN)_4]^{3-} + [^*MO(OH)(CN)_4]^{2-}$ (k_{2ex}). The values [Tc(V) results in square brackets] for the protonation and deprotonation rate constants, and the direct proton exchange rate constants in *acidic* medium (pH < 5) were determined as follows: $k_{1a} \geq 1 \times 10^8$ s^{-1} [$\geq 1 \times 10^7$], k_{2a} = 1.1(2) × 10^7 s^{-1} [1.1(5) × 10^7], k_{-2a} = 6(1) × 10^{10} M^{-1} s^{-1} [$\sim 1 \times 10^{11}$], $k_{-1a} \geq 2 \times 10^9$ M^{-1} s^{-1} [$\geq 8 \times 10^9$], and $k_{2ex} \leq 5 \times 10^7$ M^{-1} s^{-1} [$\geq 5 \times 10^8$].

Introduction

The protonation and substitution behavior of the *trans*-dioxotetracyanometalate complexes of Mo(IV), W(IV), Tc(V), and Re(V) have been described in detail in previous papers.[3,4] We have recently started exchange kinetic studies on these systems with the aid of carbon-13 and oxygen-17 NMR, of which the complete characterization study of the different species for the Re(V) system has been reported.[5] It was clear from this study that the chemical shift data and therefore the electronic environment of the coordinated oxygen ligands could be correlated directly with structural and infrared data. The Re(V) system showed that the equilibrium and kinetic behavior of these systems, in correlation with previously observed ligand substitution reactions,[3,4] can be summarized as shown in Scheme 1 (M = Re(V)). Moreover, it was concluded that the oxygen exchange

Scheme 1

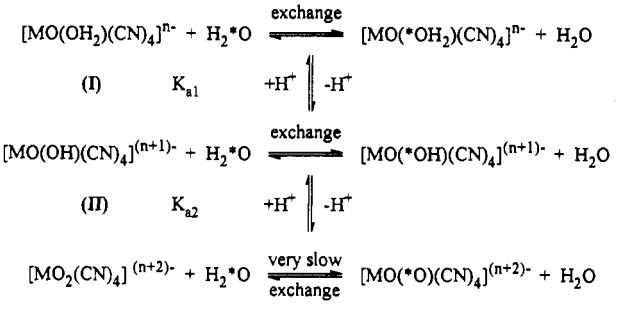

observed[5] on the oxo sites of the hydroxo and aqua complexes (not shown in Scheme 1) occurs as a result of exchange of the labile aqua ligand followed by subsequent proton exchange, which results in the enrichment of the unreactive oxo ligand. This qualitative study pointed to special characteristics in terms of ^{17}O signal behavior, specifically the fact that only one average signal was observed in going across both the protonation steps (reactions I and II in Scheme 1) of the Re(V) system and, furthermore, the substantial increase in the line width that was observed at pH values less than the pK_{a1} value (=1.31).[5] This was attributed to rapid protonation/deprotonation but was not quantified.

Earlier pioneering work by Eigen[6] showed that the exchange of a proton in aqueous acidic/basic medium between species HX and X^{*-} can in general be represented by Scheme 2. This mechanism, involving protolysis and hydrolysis (acid and base catalysis) and direct proton transfer, can be used as model for

⊗ Abstract published in *Advance ACS Abstracts*, December 1, 1993.

(1) University of the Orange Free State.

(2) Université de Lausanne.

(3) (a) Roodt, A.; Leipoldt, J. G.; Deutsch, E. A.; Sullivan, J. C. *Inorg. Chem.* **1992**, *31*, 1080. (b) Roodt, A.; Leipoldt, J. G.; Basson, S. S.; Potgieter, I. M. *Transition Met. Chem.* **1988**, *13*, 336. (c) Roodt, A.; Leipoldt, J. G.; Basson, S. S.; Potgieter, I. M. *Transition Met. Chem.* **1990**, *15*, 439 and references within. (d) Potgieter, I. M.; Basson, S. S.; Roodt, A.; Leipoldt, J. G. *Transition Met. Chem.* **1988**, *13*, 209 and references within. (e) Purcell, W.; Roodt, A.; Basson, S. S.; Leipoldt, J. G. *Transition Met. Chem.* **1989**, *14*, 224. (f) Purcell, W.; Roodt, A.; Leipoldt, J. G. *Transition Met. Chem.* **1991**, *16*, 339. (g) Purcell, W.; Roodt, A.; Basson, S. S.; Leipoldt, J. G. *Transition Met. Chem.* **1989**, *14*, 369. (h) Smit, J. P.; Purcell, W.; Roodt, A.; Leipoldt, J. G. *J. Chem. Soc., Chem. Commun.* **1993**, *18*, 1388.

(4) (a) Leipoldt, J. G.; Basson, S. S.; Roodt, A. *Advances in Inorganic Chemistry*; Sykes, A. G., Ed.; Academic Press: Talahassee, FL, 1993; Vol. 40, in press. (b) Leipoldt, J. G.; Basson, S. S.; Roodt, A.; Purcell, W. *Polyhedron* **1992**, *11*, 2277.

(5) Roodt, A.; Leipoldt, J. G.; Helm, L.; Merbach, A. E. *Inorg. Chem.* **1992**, *31*, 2864.

(6) Eigen, M. *Angew. Chem.* **1963**, *75*, 489.

0020-1669/94/1333-0140$04.50/0

Scheme 2

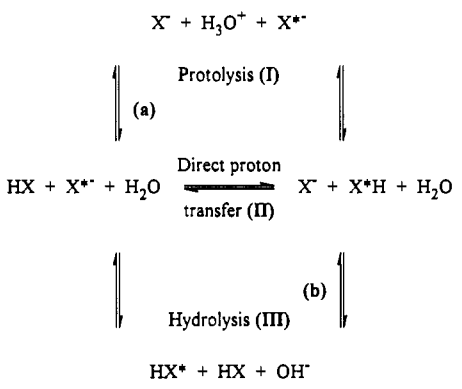

the interpretation of the H^+ exchange in these oxocyano systems. If only the acid/base proton dissociation of complex HX is considered, Scheme 2 is simplified to include only steps (a) and (b) therein. According to this model reaction I is the primary deprotonation pathway in acidic medium, while reaction III is of importance in basic media. On the other hand, direct proton transfer can occur around neutral pH values.

Our aim in this present study was to extend our NMR investigation of these systems to that of the Mo(IV), W(IV), and Tc(V) in order to get quantitative information regarding factors governing signal behavior that could not be clarified by the Re(V)[5] study alone. Using the NMR data obtained from these four similar dioxotetracyanometalates, we were able to simulate the spectra, model the proton exchanges, and obtain rate constants as described by the Eigen model in Scheme 2.

Experimental Section

General Considerations. $K_3Na[MoO_2(CN)_4]\cdot 6H_2O$, $K_3Na[WO_2(CN)_4]\cdot 6H_2O$, $K_3[TcO_2(CN)_4]$, and $K_3[ReO_2(CN)_4]$ were prepared as described previously.[3,4]

Caution! Technetium-99 emits a low energy (0.292 MeV) β-particle with a half-life of 2.12×10^5 years. When this material is however handled in milligram amounts it does not present any serious health hazard since ordinary laboratory glassware and other materials provide adequate shielding. Bremsstrahlung is not a significant problem due to the low energy of the β-particle emission, but normal radiation safety procedures must be used at all times, especially when handling solid samples, to prevent contamination and inadvertent inhalation.

Unless otherwise noted, all chemicals were of reagent grade, and all experiments were performed aerobically in aqueous medium. All measurements were performed on solutions with total metal concentration of 0.2 *m* at ionic strength of 1.0–1.4 *m* (KNO_3 supporting electrolyte) and 25 °C unless otherwise stated. A combined calomel electrode from Radiometer (GK2322C) and a Metrohm Herisau E603 pH meter were calibrated with standard HNO_3 and decarbonated NaOH in the usual way; secondary buffers were also used at intermediate pH's. The pH is defined as $-\log [H^+]$. In the pH dependence studies, microtitration on a 2 mL solution of metal complex with a micropipet and standardized 10 M NaOH, 15 M HNO_3, and 9 M HCl solutions were performed inside the NMR tube (10 mm outside diameter).

NMR Measurements. All NMR experiments were done on a Bruker AM-400 spectrometer (cryomagnet 9.4 T), at 54.227 MHz (oxygen-17) and 100.6 MHz (carbon-13). The external standard used in the ^{13}C studies was 3-trimethylsilyltetradeuteriopropionate (3TMSP), while in the case of ^{17}O the shift was referenced to the water peak and measured with respect to the nitrate ion, $\delta(NO_3^-) = 413$ ppm, as internal reference. When necessary, the free water peak was also used as a quantitative reference. All aqueous solutions used for oxygen-17 measurements contained 5% oxygen-17 enriched water. The temperature was controlled by a Bruker B-VT 1000 unit and was measured by substituting the sample tube for one containing a Pt-100 resistor.[7] In the ^{13}C study the following NMR parameters were used: over a frequency range of 22.7 kHz 16K data points were acquired at a pulse length of 20 μs. An exponential line broadening of 12 Hz was used with 1.4 s time intervals between transients, of which between 1000 and 3000 were added prior to Fourier transformation. Unless otherwise stated in the figure headings, the parameters for the general collection of ^{17}O NMR spectra were the following: A frequency range of 55.5 kHz was used to collect 2K data points with a pulse length of 15 μs and an exponential line broadening of 80–100 Hz, which was subtracted in the data analysis. The time between transients, of which between 1000 and 30000 were added prior to Fourier transformation, was 18 ms.

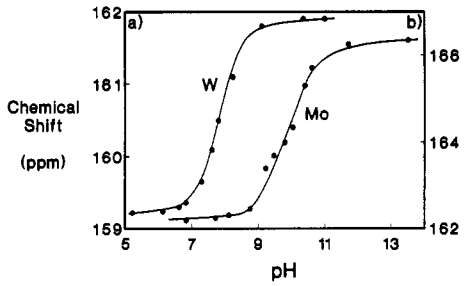

Figure 1. Influence of pH on the ^{13}C chemical shift, δ, for the (a) W(IV) and (b) Mo(IV) systems at 25.0 °C, [M] = 0.2 *m*, and μ = 1.0–1.4 *m* (KNO_3). NMR reference: 3TMSP.

Line widths and chemical shifts as a function of solution pH were obtained by computer simulation of the NMR spectra using the Kubo-Sack method.[8] The data points in the figures represent experimental values while calculated functions are given as solid lines. Dotted lines represent error limits estimated from calculations. A value for the ion product of water (K_w) of 1.5×10^{-14} (ionic strength: 1.2 M) was used throughout these calculations.[9]

The experimentally measured ^{17}O line widths in the absence of exchange used in the calculations were as follows: (i) *oxo* signals of the oxo aqua and oxo hydroxo complexes of Mo(IV) 160 (at 904 ppm) and 175 Hz (at 864 ppm) and of W(IV) 200 (at 751 ppm) and 200 Hz (at 649 ppm); (ii) *oxo* signal of the dioxo complexes of Re(V) 127 Hz (at 462 ppm) and of Tc(V) at 125 Hz (at 578 ppm); (iii) a value of 175 Hz was used as the line width for all the other ^{17}O calculations, estimated from the average observed signal width.

Results

Equilibrium Studies. As in the case of the mentioned Re(V)[5] study, we have opted for the investigation of the two Mo(IV) and W(IV) systems by carbon-13 NMR to verify previously observed protonation behavior prior to the evaluation of the more complex ^{17}O spectra. The pH dependence of the chemical shift of the ^{13}C signal for both the Mo(IV) and W(IV) systems are illustrated in Figure 1. Since there is a large difference in the pK_{a_1} and pK_{a_2} values for both the Mo(IV) and W(IV) systems, see Table 1, the pK_{a_1} value could be determined by a least-squares fit of the ^{13}C chemical shift (δ) vs pH data to eq 1. In eq 1, δ_a and δ_h represent

$$\delta = \frac{\delta_a[H^+] + \delta_h K_{a_1}}{[H^+] + K_{a_1}} \qquad (1)$$

the ^{13}C chemical shift of the aqua–oxo and hydroxo–oxo complexes respectively. The results obtained from these fits for both the W(IV) and Mo(IV) systems are reported in Table 1. The pK_a values for the Tc(V) system could not be determined by ^{13}C NMR as a result of the rapid formation of the dinuclear $[Tc_2O_3(CN)_8]^{4-}$ species whenever there were appreciable amounts of the $[TcO(OH)(CN)_4]^{2-}$ ion present.[3a]

pH Dependence of the ^{17}O NMR Spectra. The pH dependence of the W(IV) system was carefully studied over the pH range 6–14 and the effect of the pH on the line width, chemical shift, and species distribution is shown in Figures 2 and 3a–c. A significant change in signal shift from ca. 750 to 650 ppm is observed upon a pH increase from 6–8, followed by a signal

(7) Ammann, C.; Meier, P.; Merbach, A. E. *J. Magn. Reson.* **1982**, *46*, 319.

(8) Johnson, C. S.; Moreland, C. S. *J. Chem. Educ.* **1973**, *50*, 477.

(9) Smith, R. M.; Martell, A. E. *Critical Stability Constants*; Plenum Press: New York, 1976; Vol. 4, p 1.

Table 1. Summary of Acid Deprotonation Constants and NMR Data for Different $[MO(OH_2)(CN_4)]^{n-}$ Complexes at 25.0 °C and μ = 1.0–1.4 *m* (KNO_3)

param	site[a]	system			
		Re(V)[b]	Tc(V)	W(IV)	Mo(IV)
pK_{a_1}[lit]		1.31(7)	2.90(8)[c]	7.80(10)[c]	9.90(10)[c]
pK_{a_1}[d]				7.89(5)	9.88(4)
pK_{a_1}[e]				7.85(5)	9.88(5)
pK_{a_2}[lit]		3.72(5)	4[f]	14.5[c]	≫14[c]
	OMO	142			
$\delta(^{13}C)$ (ppm)	OMOH	134		162	166
	$OMOH_2$	128		159	163
	$OMOH_2$	889[g]	1055	751	904
	OMOH	759[h]	923[m]	649	816
$\delta(^{17}O)$ (ppm)	OMO	462	578	390[i]	460[j]
	OMOH	127[h]	105[m]	55	58[k]
	$OMOH_2$	−3[g]	0[i]	−17	0[i]

[a] For ^{13}C: four equivalent equatorial cyano ligands. [b] References 5. [c] References 3 and 4. [d] From ^{17}O data in Figure 3b and 4b. [e] From ^{13}C data in Figure 1. [f] See text for estimation of this value. [g] Obtained from the average observed oxo–aqua signal in water (443 ppm) and the difference (893 ppm) of the oxo and aqua signals in DMSO.[5] [h] Obtained from the average observed oxo–hydroxo signal in water (443 ppm) and the difference (633 ppm) of the oxo and hydroxo signals in DMSO.[5] [i] Estimated (±10 ppm) from the observed chemical shift at pH ca. 14.5. [j] Expected (±30 ppm) from comparison with the W(IV) and Re(V) systems. [k] Obtained from the average oxo–hydroxo chemical shift at pH ca. 13 (437 ppm) and that of the oxo signal from the oxo–hydroxo complex at pH ca. 11 (816 ppm). [l] Expected (±15 ppm) at ca. 0 ppm but not observed due to wide bulk water signal. [m] Estimated from the W(IV), Re(V), and Mo(IV) systems.

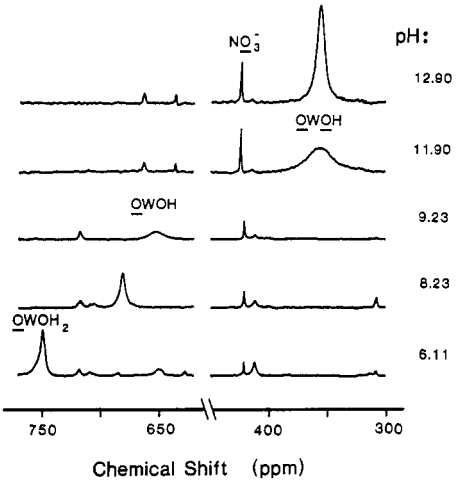

Figure 2. pH dependence of ^{17}O spectra for the W(IV) system at T = 25.0 °C, [W] = 0.2 *m*, and μ = 1.0–1.4 *m* (KNO_3). NMR reference: $H_2{}^{17}O$. For NMR parameters see Experimental Section. The spurious signals have not been identified but are partially due to the dimeric species; see ref 5.

broadening and eventual disappearance of the signal if the pH is increased from 9–10 (Figure 2). A further increase in pH (>10) results in the appearance of a signal at ca. 360 ppm. At pH = 6, where only the aqua oxo complex of W(IV) is present, the signal at 751 ppm represents the signal of the oxo site in the $[WO(OH_2)(CN)_4]^{2-}$ complex since a W:O molar ratio of approximately 1:1 is obtained, taking into account the integral (with reference to the bulk water) of the specific oxo signal and the concentration of the W(IV) used. At pH values of ca. 9 a W:O ratio of ca. 1:1 is still observed for this signal, as expected for the oxo signal of the hydroxo oxo complex. At pH > 10, the oxo signal enters the fast exchange regime with the hydroxo signal and produces an average signal for the two oxygen entities of the $[WO(OH)(CN)_4]^{3-}$ complex (W:O ratio = 1:2 under these conditions) at ca. 360 ppm; see Figure 2. The chemical shifts for the aqua and hydroxo signals of the aqua–oxo and hydroxo–oxo complexes in the slow exchange regime (pH < 9) are only just

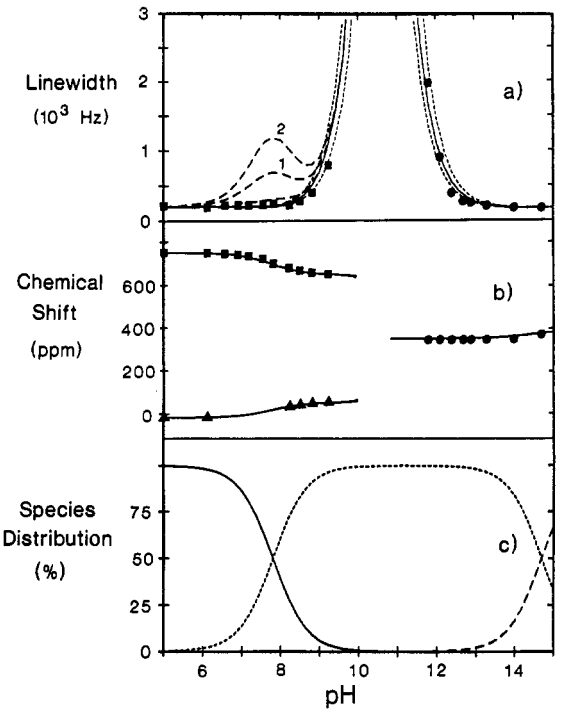

Figure 3. W(IV) system, observed and calculated pH dependence of 54.227-MHz ^{17}O signal: (a) line width (oxo (■); fast exchange (●), for dashed lines 1 and 2, see text; (b) chemical shift (oxo, (■); aqua–hydroxo (▲); fast exchange (●)); (c) species distribution ($OWOH_2$ (—); OWOH (- - -); OWO (– –)). Conditions: 25.0 °C; [W] = 0.2 *m*; μ = 1.0–1.4 *m* (KNO_3).

observed (on the side of the strong bulk water signal) at ca −17 and 55 ppm, respectively. In contrast for the Re(V) system, only an average signal resulting from the oxo and aqua sites in the $[ReO(OH_2)(CN)_4]^-$ ion (Re:O molar ratio = 1:2) could be observed over the whole accessible pH range in aqueous medium.[5]

The Mo(IV) system was also studied and the pH dependence of the signal line width, chemical shift, and species distribution is shown in Figure 4a–c. Similar signal behavior to that described above for the W(IV) was observed for the Mo(IV) system, showing a similar chemical shift dependence of the oxo signal upon increasing the pH higher than the pK_{a_1} value (9.9), allowing (as for the W(IV) system) one to accurately measure the chemical shifts and line widths of both the oxo sites in the aqua–oxo and hydroxo–oxo complexes. The chemical shifts for the hydroxo and aqua signals of the Mo(IV) system could not be measured due to the small differences with respect to the bulk aqua peak and were consequently calculated from the average observed peak for the hydroxo–oxo complex and the chemical shifts of the oxo sites measured for the aqua–oxo and hydroxo–oxo complexes; see Table 1.

The previously observed behavior[5] of the Re(V) system, that is, the pH dependence of the ^{17}O signal line width, chemical shift, and species distribution was reevaluated quantitatively, and is shown in Figure 5a–c. In the case of the Re(V) the system remains in the fast exchange regime (i.e., only an average signal is observed for the oxo and the aqua–hydroxo signals in the aqua–oxo and hydroxo–oxo complexes) in going across both the pK_a values (pH 0–7). The significant pH dependence of both the chemical shift and the line width is worth noting.

The Tc(V) system was chemically the less feasible to study as a result of the rapid formation of a dinuclear species[3a] as soon as the $[TcO(OH)(CN)_4]^{2-}$ complex is present in appreciable amounts. The few available data points for the Tc(V) system were also analyzed by means of information obtained from the other systems. The signal broadening, chemical shift, and species distribution as a function of pH are shown in Figure 6a–c.

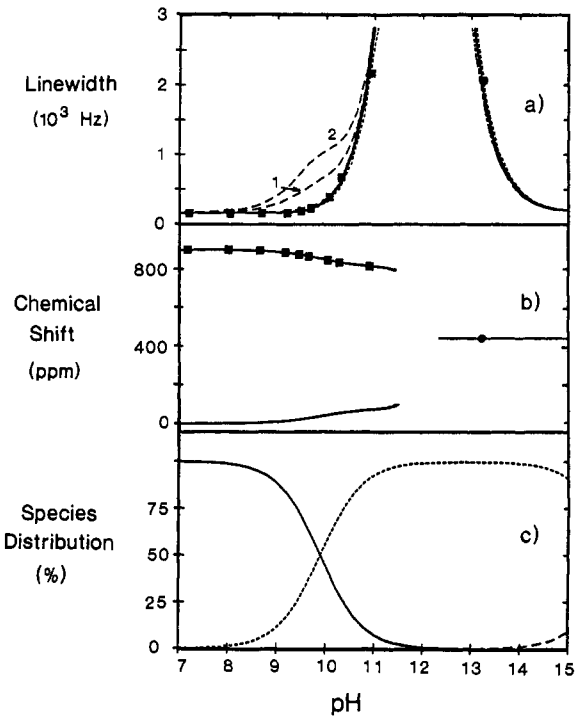

Figure 4. Mo(IV) system, observed and calculated pH dependence of 54.227-MHz ^{17}O signal: (a) line width (oxo (■); fast exchange (●)), for dashed lines 1 and 2, see text; (b) chemical shift (oxo (■); fast exchange (●)); (c) species distribution ($OMoOH_2$ (—); OMoOH (- - -); OMoO (– –)). Conditions: 25.0 °C; [Mo] = 0.2 *m*; μ = 1.0–1.4 *m* (KNO_3).

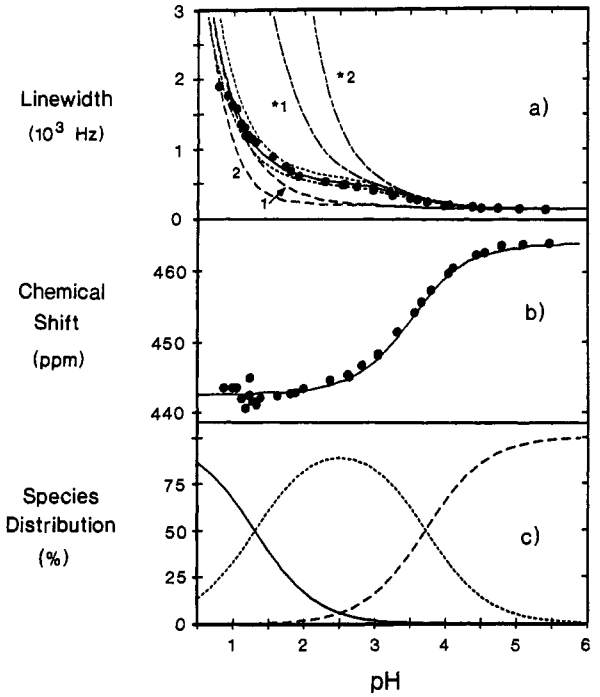

Figure 5. Re(V) system, observed and calculated pH dependence of 54.227-MHz ^{17}O signal: (a) line width (fast exchange (●)), for dashed lines 1, 2, *1, and *2 see text; (b) chemical shift (fast exchange (●)); (c) species distribution ($OReOH_2$ (—); OReOH (- - -); OReO (– –)). Conditions: 25.0 °C; [Re] = 0.2 *m*; μ = 1.0–1.4 *m* (KNO_3).

The chemical shift data of the four systems in absence of exchange are schematically summarized in Figure 7, showing the relative effect that mono- and diprotonation have on these metal centers. The oxo signals are at high frequency (ca. 700–1050 ppm), and the dioxo signals are at intermediate values (400–600 ppm), while the hydroxo and the aqua signals are close to the bulk water signal.

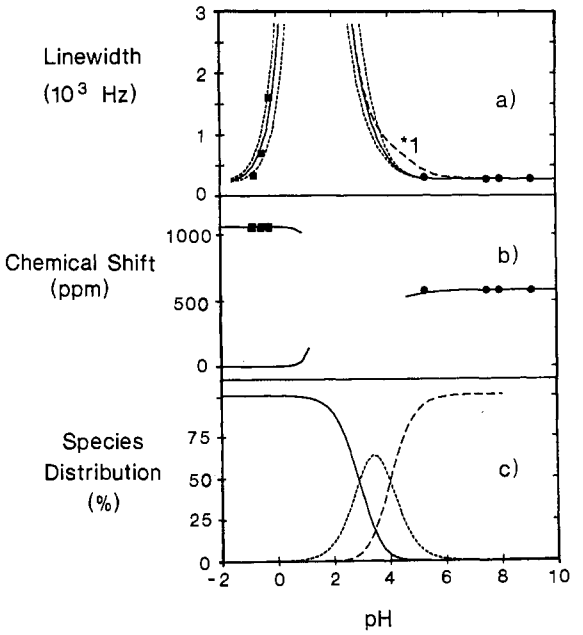

Figure 6. Tc(V) system, observed and calculated pH dependence of 54.227-MHz ^{17}O signal: (a) line width (fast exchange (●)), for dashed line *1, see text; (b) chemical shift (oxo (■); fast exchange (●)); (c) species distribution ($OTcOH_2$ (—); OTcOH (- - -); OTcO (– –)). Conditions: 25.0 °C; [Tc] = 0.1 *m*, μ = 1.0–1.4 *m* (KNO_3).

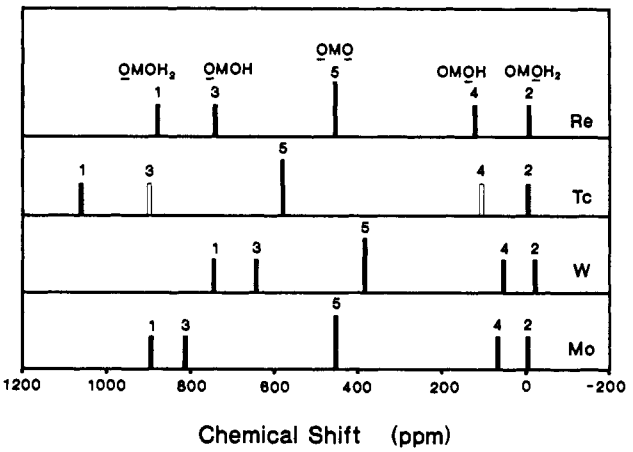

Figure 7. Oxygen-17 chemical shifts for the different sites (see eqs 2 and 3) of the Tc(V) Re(V), W(IV) and Mo(IV) systems (see Table 1; open bars are the expected values). T = 25.0 °C; μ = 1.0–1.4 *m* (KNO_3).

Exchange Matrices for Proton-Exchange Reactions. The complicated signal characteristics can be rationalized using the Eigen[6] exchange model given in Scheme 1.

(i) Basic Medium. The hydrolysis pathway (**III**) of the Eigen model in Scheme 2 describes the proton exchange in systems studied in basic media, as was the case for the Mo(IV) and W(IV) systems. The five exchange sites in these two systems are shown in eqs 2 and 3. In this case the deprotonation rates (k_{-1b} and k_{-2b})

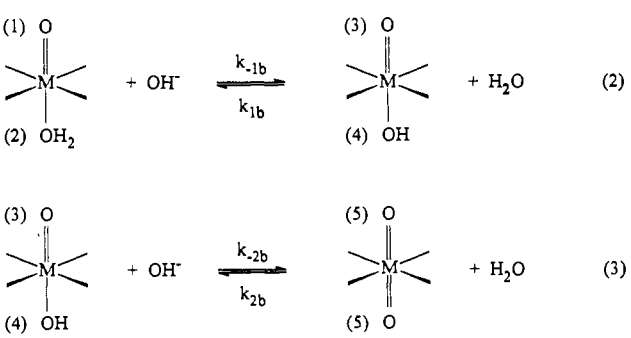

are expected to be close to diffusion controlled. The populations (p_n) of the five different sites are expressed in terms of the concentration of the different species with incorporation of the acid dissociation constants K_{a_1} and K_{a_2}, and are given by eqs 4–6. In eqs 4–6, the total metal complex concentration is denoted by [M].

$$p_1 = p_2 = [MO(OH_2)(CN)_4^-]/(2[M]) = 0.5/(1 + K_{a_1}/[H^+] + K_{a_1}K_{a_2}/[H^+]^2) \quad (4)$$

$$p_3 = p_4 = [MO(OH)(CN)_4^{2-}]/(2[M]) = 0.5/(1 + [H^+]/K_{a_1} + K_{a_2}/[H^+]) \quad (5)$$

$$p_5 = 2[MO_2(CN)_4^{3-}]/(2[M]) = 1/(1 + [H^+]/K_{a_1} + [H^+]^2/K_{a_1}K_{a_2}) \quad (6)$$

The Kubo–Sack matrices[8] describing the proton exchange between the sites in eqs 2 and 3 may consequently be constructed and can be summarized as follows (*N.B.* as a result of the five-exchange site model 5 × 5 matrices have to be considered at all times; only the nonzero nondiagonal elements are reported). The matrix elements are finally transformed to contain p_n and the **protonation** rate constants, k_{1b} and k_{2b}.

$$(1,3) = (2,4) = k_{-1b}[OH^-] = (p_3/p_1)k_{1b}$$

$$(3,1) = (4,2) = k_{1b} \quad \textbf{(matrix 1 exchange: eq 2)}$$

$$(3,5) = (4,5) = k_{-2b}[OH^-] = 0.5(p_5/p_3)k_{2b}$$

$$(5,3) = (5,4) = 0.5k_{2b} \quad \textbf{(matrix 2 exchange: eq 3)}$$

(ii) Acidic Medium. The proton exchange for systems studied in acidic medium is described by protolysis (pathway **I** in the Eigen model in Scheme 2), as was the case for the Tc(V) and Re(V) systems. In this case the protonation rate constants (k_{-1a} and k_{-2a}) are expected to be close to diffusion controlled. The exchange sites for these systems are defined in eqs 7 and 8. From

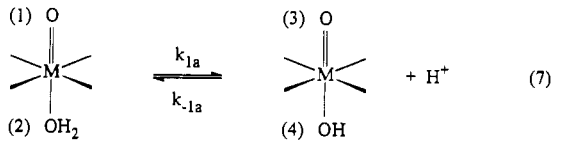

(7)

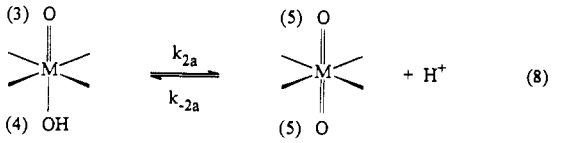

(8)

the definitions of the acid dissociation constants for the deprotonation reactions, the Kubo–Sack exchange matrices of the sites defined in eqs 7 and 8 can again be constructed and are given below. The matrices' elements are expressed in terms of known entities (p_n and K_a values) and the **protonation** rate constants, k_{-1a} and k_{-2a}.

(iii) Neutral Medium. The Eigen model in Scheme 2 also gives a third possibility for proton exchange, i.e., via direct H^+ transfer (pathway **II**). This is however only valid for systems studied around neutral pH values, where the actual $[H^+]$ and $[OH^-]$ are very small compared to the concentration of the species undergoing the proton transfer. In this case two exchange processes as illustrated by eqs 9 and 10 can be visualized to describe

$$(1,3) = (2,4) = k_{1a} = k_{-1a}K_{a1}$$

$$(3,1) = (4,2) = k_{-1a}[H^+] = (p_1/p_3)k_{-1a}K_{a1} \quad \textbf{(matrix 3 exchange: eq 7)}$$

$$(3,5) = (4,5) = k_{2a} = k_{2a}K_{a2}$$

$$(5,3) = (5,4) = 0.5k_{-2a}[H^+] = (p_3/p_5)k_{-2a}K_{a2} \quad \textbf{(matrix 4 exchange: eq 8)}$$

the proton transfer between the three different species in the four systems of the current study. Equation 9 describes the direct exchange relevant in the Mo(IV) and W(IV) systems while eq 10 has to be considered for the Tc(V) and Re(V). Upon

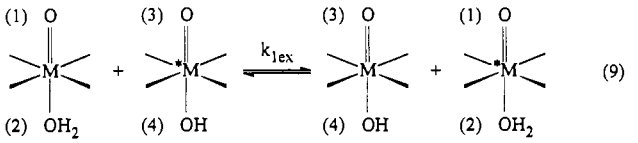

(9)

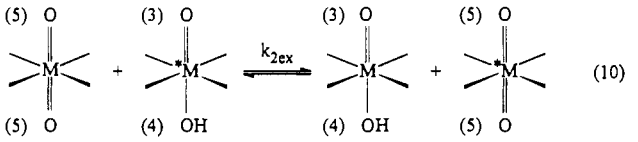

(10)

incorporation of the population definitions as given in eqs 4–6, the relevant Kubo–Sack exchange matrices can again be constructed and are given below for the direct proton transfer illustrated in eqs 9 and 10. The notations of [OMO], [OMOH], and [$OMOH_2$] represent the concentration of the dioxo, hydroxo–oxo, and aqua–oxo complexes, respectively.

$$(1,3) = (2,4) = k_{1ex}[OMOH] = 2k_{1ex}p_3[M]$$

$$(3,1) = (4,2) = k_{1ex}[OMOH_2] = 2k_{1ex}p_1[M] \quad \textbf{(matrix 5 exchange: eq 9)}$$

$$(3,5) = (4,5) = k_{2ex}[OMO] = k_{2ex}p_5[M]$$

$$(5,3) = (5,4) = 0.5k_{2ex}[OMOH] = k_{2ex}p_3[M] \quad \textbf{(matrix 6 exchange: eq 10)}$$

Determination of Proton Exchange Rate Constants. The experimentally determined chemical shift and line width data in the absence of exchange for the aqua–oxo, hydroxo–oxo, and dioxo species (Table 1) and the pH-dependent species distribution as calculated from the acid dissociation constants for the four systems were all introduced in the different matrices and the spectra were simulated by computer. For each set of chosen rate constants (two or three) the pH dependence of the shifts and line widths (one or two signals) were represented graphically and visually compared to the experimental data (Figures 3–6). The results are described below and the rate constants thus obtained are reported in Table 2.

(i) Tungsten(IV). Since this system was studied in basic medium the combination of matrices 1 and 2 were introduced in the computer simulations (see solid lines in Figure 3a and b) which used the deprotonation rate constant values k_{1b} and k_{2b} (see eq 2 and 3) reported in Table 2. The effect of variation of k_{-2b} (± 30%) on the line widths is represented by the short dashed lines. At very high pH the simulations started deviating significantly from the experimental data when a pK_{a_2} value of

Table 2. Proton Exchange Rate Constants Obtained from the Simulation of the Data in Figures 3–6

rate constants[a]	value[b] Mo(IV)	W(IV)
k_{-1b}[c]/s^{-1}	not defined	not defined
k_{-2b}[d]/M^{-1} s^{-1}	1.3(2) × 10^9	7(2) × 10^8
k_{2b}[e]/s^{-1}	2(1) × 10^7	4(2) × 10^8
k_{1ex}/M^{-1}/s^{-1}	≥1 × 10^7	≥1 × 10^7

rate constants[a]	value Tc(V)	Re(V)
k_{1a}[d]/s^{-1}	≥1 × 10^7	≥1 × 10^8
k_{-1a}[f]/M^{-1} s^{-1}	≥8 × 10^9	≥2 × 10^9
k_{2a}[d]/s^{-1}	1.1(5) × 10^7	1.1(2) × 10^7
k_{-2a}[f]/M^{-1} s^{-1}	1.0(4) × 10^{11} [g]	6(1) × 10^{10}
k_{2ex}/M^{-1} s^{-1}	≥5 × 10^8	≤5 × 10^7

[a] See eqs 2, 3, 7, 8, 9, and 10. [b] For values reported with ≥ and ≤ only limits could be estimated. [c] Can take any value, see text. [d] In protolysis (eqs 7 and 8) and hydrolysis (eqs 2 and 3) reactions either the forward k or the reverse k_- rate constant is best defined (or a limit is given) by the ^{17}O NMR line-broadening data, while the other depends on the related acid dissociation constant (which may be well-defined or not). This value gives the best defined constant while the error reported for the reverse reaction takes into account the uncertainly on the acid dissociation constant. [e] Calculated, $k_{-2b} = k_{2b}K_{a_2}/K_w$, assuming pK_{a_2} = 14.5 and 16.0 for W(IV) and Mo(IV) respectively. [f] Calculated, $k_{ra} = k_{-ra}K_{a,n}$, n = 1, 2; Table 1. [g] Value obtained using a pK_{a_2} value of 4 (the quoted error comes from the least-squares fit). Considering the uncertainty on pK_{a_2}, the value of k_{-2a} is only approximate: 1 × 10^{11} M^{-1}s^{-1}. See text for estimation of pK_{a_2}.

less than 13 was included in the calculations, confirming that the pK_{a_2} value for the W(IV) system is > 13.

For k_{1b} only a lower limit could be given. The long dashed lines in Figure 3a show the effect of a decrease (curve 1, 1 × 10^5, and curve 2, 5 × 10^4 s^{-1}) in k_{1b} below this limit (1 × 10^6 s^{-1}). This leads to an unrealistic k_{-1b} value, $k_{-1b} = k_{1b}K_{a_1}/K_w \geq 2 \times 10^{12}$ M^{-1} s^{-1}, and therefore suggests another exchange pathway to be operative at the intermediate pH values, i.e., a direct proton exchange.

To test the operation of this direct proton exchange pathway, the combination of matrices 1, 2, and 5 was used. Within this model the value obtained for the constant k_{2b} in the second deprotonation equilibrium (eq 3) is unchanged. Furthermore, a limiting value for the direct proton transfer constant, k_{1ex}, is obtained, which describes the proton exchange at intermediate pH values. The variation of k_{1ex} is shown in Figure 3a, which essentially results in the same calculated function shown by the dashed line 1 (1 × 10^6 M^{-1} s^{-1}) and 2 (1 × 10^5 M^{-1} s^{-1}), allowing the determination of the minimum value reported in Table 2. The significance of the different exchange pathways are discussed later.

(ii) Molybdenum(IV). Since the Mo(IV) system was also studied in basic medium, the chemical shift and line broadening data obtained were evaluated similar to those obtained for the W(IV) system, i.e., by means of both matrix combinations (1,2 and 1,2,5). The results from the computer simulations of the data are illustrated in Figure 4a (line width) and Figure 4b (chemical shift), and the proton exchange constants are reported in Table 2. The two systems (W(IV) and Mo(IV)) behave quite similarly (Figures 3 and 4), and the same arguments therefore hold for both. The value of k_{2b} reported by this simulation is obtained with a ±10% (short dashed lines in Figure 4a denote error limits) accuracy (Table 2).

Assuming the process illustrated in eq 2 for Mo(IV), a lower limit of 1 × 10^7 s^{-1} for k_{1b} is obtained, and the values approaching this limit are shown in Figure 4a: curve 1 (1 × 10^5 s^{-1}) and curve 2 (5 × 10^4 s^{-1}). Therefore, in the case of the Mo(IV) as well, calculation of the proton dissociation constant (k_{-1b} in eq 2), results in an unrealistic value of $k_{-1b} = k_{1b}K_{a1}/K_w > 2 \times 10^{11}$ M^{-1} s^{-1}, suggesting that another mechanism is operative for proton exchange at the intermediate pH values.

Upon introduction of the direct exchange mechanism, a lower limit for the direct proton exchange rate constant is obtained, in line with the W(IV) system (Table 2). The variation of k_{1ex} is again illustrated by the dashed lines 1 (1 × 10^6 M^{-1} s^{-1}) and 2 (5 × 10^5 M^{-1} s^{-1}) in Figure 4a and shows that the system behaves similarly to the W(IV) system described above.

(iii) Rhenium(V). The Re(V) system was quantitatively studied in acidic medium to include NMR measurements across both pK_a values. The data were therefore analyzed by means of the combination of matrices 3 and 4, and the rate constants as defined in eqs 7 and 8 (protolysis; pathway 1 in Scheme 2) are reported; see Table 2. The computer-simulated curves and the experimental data are shown in Figure 5a (line width) and Figure 5b (chemical shift).

The rate constants obtained from the computer calculations as given in Table 2 indicate that the substantial broadening observed (at pH values less than 1 for the Re(V)) is primarily a function of k_{-2a} and k_{-1a}. An accurate value for k_{-2a} is obtained (see ±20% error limits denoted by the short dashed lines in Figure 5a). On the other hand, only a lower limit for k_{-1a} is obtained, (see converging simulations *1 (1 × 10^8 M^{-1} s^{-1}) and *2 (2 × 10^7 M^{-1} s^{-1})), when the calculated function corresponds to the experimental data. Since the pK_{a_2} value is very accurately known in this case, both the forward (k_{2a}) and reverse (k_{-2a}) rate constants in eq 8 could therefore be obtained accurately.

The magnitude of k_{-2a} for the Re(V) system obtained from the computer fit was fairly large[10] (6 × 10^{10} M^{-1} s^{-1}), and a direct exchange pathway for this proton-transfer process, similar to the W(IV) and Mo(IV) systems, was therefore also evaluated. The Re(V) system however differs in this regard significantly from the W(IV) and Mo(IV) systems described above in so far as the proton exchange between the dioxo and the hydroxo–oxo complexes (eq 10) had to be reevaluated in terms of the direct proton-transfer process. The possible direct pathway for this proton exchange step was evaluated by introducing the combination of matrices 3, 4, and 6, and the results are reported in Table 2. Figure 5a (curve 1; 5 × 10^9 M^{-1} s^{-1}, and curve 2, 5 × 10^{10} M^{-1} s^{-1}) shows the effect of variation of k_{2ex} on the simulated line width. It is clear that only an upper limit is obtained. Introducing this third exchange pathway does not change the values of k_{-2a}, which is well-defined by the experimental data, and does not modify the limiting value for k_{-1a}.

(iv) Technetium(V). The Tc(V) system was quantitatively studied in acidic medium; however, NMR measurements across both the pK_a values were not possible as a result of the rapid formation of the dinuclear species, $[Tc_2O_3(CN)_8]^{4-}$, from the hydroxo–oxo complex, as mentioned above. Consequently, only solutions where the dioxo (pH > 5.5) and aqua–oxo (pH < 2) complexes of the Tc(V) were present could be studied. At pH values of ca. 0–2 the average aqua–oxo signal of the $[TcO(OH_2)(CN)_4]^-$ is very broad and could not be observed. However, at [H$^+$] > 1 m the proton exchange between the aqua and oxo sites in the aqua–oxo complex decreases and the oxo signal of the $[TcO(OH_2)(CN)_4]^-$ complex is detected, enabling the measurement of the linewidth and chemical shift. The data could be analyzed by means of the combination of matrices 3 and 4, and the rate constants as defined in eqs 7 and 8 were obtained, see Table 2. Figure 6a shows the variation in k_{-2a} (dotted lines: ±40%). The limited data available resulted in larger error limits than the other systems. The variation in k_{-1a} has however little effect on the simulated results (not shown in Figure 6). The computer simulation of the experimental data are shown in Figure

(10) No protonation of the cyano ligands could be detected from chemical shift data within the pH ranges of the proton exchange kinetic studies (for W(IV) and Mo(IV), see Figure 1; for Re(V) down to [H$^+$] = 1 M, see ref 5; for Tc(V) between 1 and 6 M [H$^+$] and above pH 4, see Figure 6).

6a (line width) and Figure 6b (chemical shift) and the results are reported in Table 2. The same exchange process as described above for the Re(V) system adequately describes the proton transfer in the Tc(V) system, and the effect of a direct proton-exchange pathway (eq 10) between the dioxo and hydroxo–oxo species was evaluated by introduction of matrices 3, 4, and 6. The effect of the variation of k_{2ex} is shown in Figure 6a: curve *1 (1×10^8 M^{-1} s^{-1}). In contrast with the Re(V) system, the data available allowed not a maximum, but a minimum value for the direct exchange constant to be obtained.

Discussion

Chemical and Equilibrium Studies. The pK_a values obtained from the ^{13}C pH dependence studies (Figure 1) for the Mo(IV) and W(IV) systems are in excellent agreement with the previously determined acid dissociation constants for these $[MO(OH_2)(CN)_4]^{(n+2)-}$ complexes, as shown in Table 1.

The ^{13}C and ^{17}O (Figure 7) chemical shift data for the signals of the individual sites included in Table 1 are determined by the electronic environment of the coordinated cyano and oxygen ligands and can in turn be correlated with the Lewis acidity of the metal centers. The ^{17}O chemical shifts for the signals of the oxo ligands in both the $[MO(OH)(CN)_4]^{(n+1)-}$ and $[MO(OH_2)(CN)_4]^{(n+2)-}$ complexes in Table 1 suggest that the ability of the metal center to accept electron density from the oxo ligand is in the order Tc(V) > Mo(IV) > Re(V) > W(IV). This results in M=O "cores" for which the Lewis acidity trans to the oxo is (Re=O) > (Tc=O) > (W=O) > (Mo=O); see pK_{a_1} and pK_{a_2} values in Table 1. However, it is clear that the effect of the metal center on the cyano ligands cis to the oxo ligand, as obtained from the ^{13}C data, shows a different order: Mo(IV) > W(IV) > Re(V). (Since no ^{13}C data was obtained for the Tc(V) compound, comparison with the other systems is not possible.) This suggests that the carbon atoms of the cyano ligands coordinated to the Re(V) center are more electron-rich than those coordinated to the W(IV) center and in turn that of W(IV) more than the cyano ligands of the Mo(IV). This is in agreement[11] with proton NMR data obtained for corresponding Re(V) and Tc(V) complexes, where it was shown that ligands coordinated cis to the oxo ligand in these centers experience more interaction with the metal atom in the case of Tc(V) than Re(V). This is also in line with the above mentioned effect of the metal center on the oxo ligand, as well as the fact that the third row metals are more difficult to reduce than their corresponding second row congeners.

Protonation of an oxo ligand in any of these four metal systems results in electron density changes on the metal centers in the protonated complexes. The decrease in electron density on any one oxo ligand upon protonation of the other oxo ligand trans thereof is clear from the ^{17}O chemical shifts for all four metal systems, see Table 1 and Figure 7. On the other hand, protonation in these systems results in an increase in the trans M=O bond strength as was shown crystallographically,[3,4] which in turn also results in an increase in electron density on the cyano carbon atoms as observed from the ^{13}C chemical shifts given in Table 1. Protonation furthermore also results in a significant distortion of the coordination polyhedron; i.e., the metal ion is displaced from the plane formed by the four cyano ligand carbon atoms toward the oxo along the M=O axis by as much as 0.35 Å, which represents about 20% of the total metal–oxo bond length. In spite of this distortion, stronger metal–cyano bonds are observed crystallographically,[3,4] suggesting a better π back-donation by the metal center to the cyano carbons since d–π^* overlap is increased. This observation is in line with ^{13}C chemical shift data for the protonated complexes; see Table 1.

Proton Exchange. The actual mechanism of proton transfer in these systems can be explained in terms of the Eigen model (Scheme 2) by either hydrolysis (Mo(IV) and W(IV)) or protolysis (Tc(V) and Re(V)) pathways, coupled with direct proton transfer in the intermediate pH range. The reverse rate constants are calculated from the pK_a values and are summarized in Table 2 for comparative purposes.[10]

The proton exchange for the Mo(IV) and W(IV) systems are discussed first. The results obtained from evaluation of the systems by both the hydrolysis (**I** in Scheme 1) and hydrolysis/direct proton transfer (**I** and **II** in Scheme 1) pathways indicate that the proton exchange can be explained most convincingly by the second alternative. The overall process can therefore be summarized to proceed via hydrolysis (eq 3) in strong basic medium and via direct proton transfer (eq 9) in weak basic solution. The deprotonation of the O=M—OH moiety to form the O=M=O core is ca. 1 order of magnitude more rapid for W(IV) than for Mo(IV) (Table 2), which is in agreement with the acidity of the –OH function (in the $[MO(OH)(CN)_4]^{3-}$ complexes) of the W(IV) and Mo(IV) systems. The limits determined for the direct proton exchange rate constant, k_{1ex}, for the two systems are comparable as might be expected since the acidity characteristics of the two systems are quite similar.

The results obtained for the proton transfer reactions for the Re(V) system as described in Scheme 1 proceed in strong acid via protolysis (eq 7) and in weak acid medium via both protolysis (eq 8) and direct proton transfer (eq 10). The value for k_{2a} of 1.1×10^7 s^{-1} is well-defined, resulting in an accurate calculation for the k_{-2a} value of 6×10^{10} M^{-1} s^{-1}, since the pK_{a_2} value for the Re(V) system is accurately known; see Table 1. This k_{-2a} value is very high but in principle possible.[12] Upper limiting values for both the k_{-1a} and k_{2ex} were obtained that are of acceptable magnitude.

The results for the proton-transfer reactions for the Tc(V) system are similar to that of the Re(V) in the sense that the transfer proceed via protolysis and direct proton transfer (eq 7, 8 and 10). The value of k_{2a} of 1.0×10^7 s^{-1} is well-defined by the NMR data. Since the pK_{a_2} value for the Tc(V) system is not accurately known (as a result of the rapid[3a] formation of the dinuclear species $[Tc_2O_3(CN)_8]^{4-}$) and was estimated to be ca. 4–5; a similar uncertainty is reflected in the k_{-2a} value. Using $pK_{a_2} = 4$, a value for k_{-2a} 1×10^{11} M^{-1} s^{-1} is calculated, which is very high, but acceptable if the few data points for the Tc(V) system as well as the uncertainty in the pK_{a_2} is considered. Limiting values for k_{-1a} and k_{2ex} were again obtained, as in the case of Re(V). Of significance is the fact that a lower limit for the direct exchange constant for Tc(V) is obtained, whereas in the case of the Re(V) an upper limit could be calculated. This is fortunate and allows us, because we do not expect a large difference in behavior for the Tc(V) and Re(V) complexes, to accept the limiting values of k_{2ex} of 5×10^8 and 5×10^7 M^{-1} s^{-1}, respectively, as being close to the real rate constants.

The above-mentioned proposed *direct* proton exchange pathway (step **II** in the Eigen model[6] in Scheme 2), is likely considering the existence of dimeric species with the linear O=M—O—M=O orientation for all four[3] the metal systems investigated in this study. The formation of such species requires the association of two of the metal centers in a way that might exactly be what is required for direct proton transfer. Furthermore, different literature examples of metal complexes[13] i.e., [-Rh(en)$_2$-

(11) (a) Helm, L.; Deutsch, K.; Deutsch, E.; Merbach, A. E. *Helv. Chim. Acta* **1992**, *75*, 210. (b) Tisato, F.; Mazzi, U.; Bandoli, G.; Cros, G.; Dardieu, M.-H.; Coulais, Y.; Guiraund, R. *J. Chem. Soc., Dalton Trans.* **1991**, 1301.

(12) The diffusion-controlled rates for protonation of a base by H^+ in water are of the order of 4×10^{-10} M^{-1} s^{-1} at 25 °C in water (Jordan, R. B. *Reaction Mechanisms of Inorganic and Organometallic Systems*; Oxford University Press: New York, 1991; p 21).

(13) (a) Ardon, M.; Bino, A. *Inorg. Chem.* **1985**, *24*, 1343. (b) Van Eldik, R.; Roodt, A.; Leipoldt, J. G. *Inorg. Chim. Acta* **1987**, *129*, 141. (c) Durham, B.; Wilson, S. R.; Hodgson, D. J.; Meyer, T. J. *J. Am. Chem. Soc.* **1980**, *102*, 600.

$(H_3O_2)(en)_2Rh-]$ and $[[M_3O_2(O_2CC_2H_5)_6(H_2O)_2]_2(H_3O_2)]^{3+}$ [14] (M = Mo, W), are known which confirms the existence of metal centers bridged by the $-(H_3O_2)-$ moiety. It is consequently also considered likely for such an intermediate (i.e. in eq 9) to exist in aqueous solutions of the aqua–oxo–tetracyano systems of the four metals investigated in this study, allowing for a direct proton-transfer process.

The values obtained for the proton transfer in these four systems (Table 2) are typical for that expected for these rapid processes. Examples from the literature where similar reactions were studied in metal complexes include the $[Cr(OH)(OH_2)]^{2+}$ [15] and $[VO(OH_2)_5]^{2+}$ [16] systems. In the proton-exchange study of the hexaaqua aluminum(III) system, a bimolecular process, similar to that proposed for the systems in this study, for the exchange between the $[Al(OH_2)_6]^{3+}$ and $[Al(OH_2)_5(OH)]^{2+}$ [17] complexes, was postulated.

The results from the Mo(IV) and W(IV) systems in this study showed a dramatic ^{17}O signal dependence on pH, changing from a fast exchange regime at high pH (increased concentrations of the $[MO_2(CN)_4]^{4-}$ ion present), with only a coalescent signal (average of oxo and hydroxo) observed, to a slow exchange regime, where two signals (both oxo and hydroxo) are observed; see Figures 3 and 4. For the Re(V) system however, only the fast exchange region is observed (Figure 5) as a result of the strong acid character of the $[ReO(OH_2)(CN)_4]^-$ complex (Table 1). Of significance is the fact that in the case of the Tc(V) system, the slow exchange regime was just accessible at $[H^+]$ = 1–10 M (Figure 6), since the $[TcO(OH_2)(CN)_4]^-$ ion is a weaker acid (Table 1) than the corresponding Re(V) complex. In fact, it was calculated by simulation of the Re(V) system that the slow exchange regime should be observed at pH ca. –2, i.e., $[H^+]$ = 100 M, and therefore is *not* accessible. Analysis and study of the Tc(V) system has therefore confirmed that the signal behavior observed in the rhenium system was in fact correct, but it was previously difficult[5] to explain with only the results for the Re(V) available.

This study showed that the oxo sites in these type of complexes are enriched as a result of H_2O/OH^- exchange followed by deprotonation/protonation. A significant observation is the fact that enrichment of the oxo site of the oxo–aqua complexes has to proceed via the dioxo complex. The concentration of the dioxo complex, coupled with the proton exchange thereof, therefore acts as a "bottleneck" and determines primarily the pH dependence of the systems entering the fast/slow exchange regimes. It is interesting to note that all the systems exit from the fast exchange regime at approximately 2 pH units below the pK_{a_2} value.

It has been shown previously by crystal structure determinations and kinetic studies that protonation of the hydroxo–oxo complex results in the formation of the aqua–oxo complex rather than the dihydroxo species.[3,4] The existence of a symmetrical dihydroxo species in solution, even as an intermediate, is consequently also ruled out by this study since the observed exchange scheme would be altered significantly. No coalescent signals would in such a case be observed since the system will always be in fast exchange with regard to proton exchange. The dihydroxo complex acting as "bottleneck" would not show the pronounced effect as was observed in this study.

The geometrical changes of the coordination polyhedron during protonation, as mentioned above in these systems, is a dynamic process, and the proton transfer in these systems is actually responsible for the inversion or oscillation rate of the metal center along the M=O axis. The driving force for the inversion in this study is obviously the actual proton transfer, however, systems might be designed to restrict such an inversion process sterically, and electronically. We plan future studies to investigate this phenomenon, which will include theoretical calculations on the dynamics of such processes.

In conclusion, oxygen-17 NMR line-broadening provides the unique opportunity to study very fast proton-transfer reactions on these metal–oxocyano complexes by lowering the concentration of the reacting species through pH manipulation.

Acknowledgment. Financial support for this project, provided by the Swiss National Science Foundation (Grant No. 20-27848.89), is gratefully acknowledged. A.R. and J.G.L. also thank the South African FRD and the Research Fund of the University of the Orange Free State for financial assistance.

(14) Bino, A.; Gibson, D. *J. Am. Chem. Soc.* **1981**, *103*, 6741.
(15) Melton, B. F.; Pollack, V. L. *J. Phys. Chem.* **1969**, *73*, 3669.
(16) Copenhafer, W. C.; Rieger, P. H. *Inorg. Chem.* **1977**, *16*, 2431.
(17) Fong, D.-W.; Grunwald, E. *J. Am. Chem. Soc.* **1969**, *91*, 2413.